UCRL - 77202
PREPRINT
Conf-751108--18

LAWRENCE LIVERMORE LABORATORY
University of California / Livermore, California

ELECTRON BEAM ENERGY DEPOSITION AND VUV EFFICIENCY MEASUREMENTS IN RARE GASES

C. E. Turner, Jr., P. W. Hoff*, and J. Taska

November 1975

This paper was prepared for submission to
International Topical Conference on Electron Beam Research and Technology
November 3-5, 1975 Albuquerque, New Mexico

* Present address: U.S. ERDA, Division of Military Applications, Washington, D.C.

ELECTRON BEAM ENERGY DEPOSITION AND VUV EFFICIENCY MEASUREMENTS IN RARE GASES

C. E. Turner, Jr., P. W. Hoff and J. Taska
Lawrence Livermore Laboratory, Livermore, CA 94550

ABSTRACT

ELECTRON BEAM ENERGY DEPOSITION AND VUV EFFICIENCY MEASUREMENTS IN RARE GASES*

C. E. Turner, Jr., P. W. Hoff and J. Taska
Lawrence Livermore Laboratory, Livermore, CA 94550

Reliable techniques for the determination of the energy/cm^3 deposited by an e-beam into a gas as well as the energy/cm^3 radiated have been developed in order to obtain dependable data on the VUV fluorescence efficiency for rare gas excimers. Spatially resolved total stopping calorimetry in the gas at the cell foil was used to characterize the energy distribution in the e-beam (~ 200 kV, few Amp/cm^2, ~ 1 μsec) transmitted by a "hibachi"-supported 1-mil Ti foil. By using this data, suitable input for a 3-D Monte Carlo electron transport code (SANDYL) was generated. The spatial distribution of energy deposition in the gas was then calculated taking into account multiple scattering and cell geometry. The validity of the SANDYL technique is substantiated by excellent agreement between the measured and calculated energy flux on a vertical stack of five fast risetime (< 1 msec) calorimeters at several depth positions [0 < Z(cm) < 15] in the gas [1 < P(atm) < 3]. Calibrated optical components were used in a well defined geometry that permitted calculation of the effective radiating volume observed. By using the above techniques, high absolute efficiencies (10-30%) have been measured for rare gas VUV continua emission which can photolytically produce group VI metastables [e.g.,$O(^1S)$,$S(^1S)$] of interest as fusion visible-laser candidates.

---

* Work performed under the auspices of the U.S. E.R.D.A. under Contract No. W-7405-Eng-48

Reliable fluorescence efficiency measurements in electron pumped gases are extremely important for development of practical lasers and very difficult to achieve. Furthermore, many "estimates" found in the scientific literature are totally inadequate for intelligent laser scaling decisions. In this paper we describe generally applicable techniques which have been used with considerable success to impact this problem.

Our initial objectives were to measure the VUV fluorescence efficiency of e^--beam produced rare gas excimers (Ar_2^*, Kr_2^*, Xe_2^*) at lower pressure (1 to 3 atm), lower energy deposition (10-50 mJ/cm^3), and longer pump times (a few μsec) than typical of xenon, krypton, and argon lasers. These conditions ameliorate some phenomena which severely limit the efficiency of such lasers. The lower excited state density reduces Penning ionization. The lower energy deposition holds down the gas temperature. With longer pump times we hope to optimize the integrated VUV fluorescence and its production efficiency at useful photon emission rates. Furthermore, utilization of the medium as a fluorescer rather than as a laser would reduce photoionization losses.

We are motivated in our pursuit of these particular systems by the synergistic effect of three important factors. First, there are high experimental efficiencies quoted for excitation by 5.3 MeV α-particles[1] or 10-30 keV electrons[2] in the condensed phase as well as by 4 MeV protons[3] in the gas phase. Secondly, high efficiencies are predicted for our intended operating conditions by a kinetic model[4] that has successfully predicted fluorescence and laser characteristics in high pressure xenon and krypton. And, finally, there is a plausible application for a fusion laser based on

photolytic production of group VI metastables [e.g., $O(^1S)$, $S(^1S)$] at high quantum yield.[5-8]

The desired quantity is the absolute VUV fluorescence efficiency, a deceptively simple ratio of radiated energy per unit volume to electron beam energy deposited per unit volume. To obtain this quantity reliably we have carefully attacked both the numerator and denominator. In this paper we first describe our optical techniques; next present, in detail, our approach for determining the spatial distribution of the electron beam energy deposition in a gas cell; and lastly give some results of the application of these techniques.

For the efficiency numerator, we measured the energy radiated from a well defined volume. We chose the optical axis such that there was minimum spatial variation of the energy deposited along the axis since there is no convenient method of achieving spatial discrimination along the optical axis for extended radiators. An evacuated light pipe was separated from the gas cell by a MgF_2 window. The light pipe contained an ITT F4115 photodiode, an aperture, scatter baffles, and in some cases a MgF_2 lens. The detector and MgF_2 optics were carefully calibrated and protected from contamination by use of a liquid nitrogen cold trap.

We also took care to avoid systematic error in calculating the effective radiating volume by comparing data from double-aperture and lens-aperture systems. A double aperture arrangement with 3.2 mm radii was used for the final results since it offered several advantages. One less transmission calibration was required. It eliminated errors associated

with focal length uncertainty and variation of focal length with wavelength. It permitted one aperture to be located at the plane of a cell wall in the gas, thereby protecting the MgF_2 window from unnecessary electron and VUV bombardment. This location also improved field of view definition for calculation of the effective radiating volume and the average energy deposited per unit volume.

Scattered light which was a significant effect even in the VUV was minimized by insertion of several baffles into the optical system and blackening the apertures and evacuated light pipe walls.

The spectral distribution of radiation was limited by the ITT F4115 photodiode to the 1100 to 3200 Å region. The portion of the optical signal transmitted through air was typically less than 7% and subtracted out on a multishot-average basis. Photographic spectra confirmed that the emission was mainly from the expected VUV excimer bands.

To obtain the efficiency denominator we have chosen a technique which avoids the pitfall of assuming that electrons travel a straight line path losing energy in a one dimensional fashion according to the tabulated Berger and Seltzer stopping powers.[9] We experimentally determined the beam spatial profiles and fluence (J/cm^2) on the gas side of the cell foil. These data were then input to a sophisticated computer code SANDYL[10] which calculated the spatial distribution of energy deposition by following electrons as they lose energy on a complicated three dimensional path. In addition, we have verified the applicability of the SANDYL code in our operating regime by detailed calorimetry versus position along the longitudinal (horizontal) e^--beam axis in the gas.

The electron beam source consisted of a two stage Marx bank with a tantalum blade cold cathode pictured in Fig. 1A. Under typical operating conditions the electrons entered the gas with an average energy of about 205 keV after losing 30 keV in a 1 mil (25 micron) titanium foil. The voltage rise and fall times were of the order of 10 nsec but the current risetime was about 1 μsec. The current into the gas cell fell essentially with the voltage. The average current density over the (10 x 100) cm^2 cathode and one μsec pulse duration was about 2.5 Amp/cm^2. Diode voltage droop during the pulse was only about 7% since most of the stored energy was crowbarred. The output capacitance and maximum output voltage were 0.375 μf and 300 kV, respectively. The usual charge voltage was 130 kV.

The calorimetric verification of SANDYL and fluorescence measurements were performed using the (15 x 15 x 100) cm^3 gas cell pictured in Fig. 1B. The foil and its support structure are removed to show the translatable calorimeter mount. Figures 2A and 2B show, respectively, the vertical and horizontal calorimeter arrays used to determine the corresponding beam fluence distribution. The arrays feature calorimeters that are essentially levitated and thermally isolated to facilitate clean data analysis and computer modeling. These calorimeters had submillisecond risetimes that were required to separate e⁻-beam deposited energy from gas heating effects at depths approaching the effective electron range. The maximum temperature rise on the 16 mm square by 0.43 mm thick Al calorimeters was about 10°K.

Some of the features of the SANDYL code that make it such a powerful tool are that it treats energy loss and deposition by electrons in three dimensions and includes an enormous amount of physics implemented via a hybrid combination of Monte Carlo and analytical techniques. For example, it treats energy loss to atomic electrons, scattering from screened atomic nuclei, and generation and tracking of energetic secondaries. It accounts for the energy variation of the stopping power and cross sections. Radiation phenomena are also included. The energy, angular, and spatial distributions of the beam electrons can be specified to the required degree of realism. In addition, effects such as absorption, scatter, and backscatter associated with realistic gas cell construction (foil, foil support, and walls) can be incorporated.

Collective phenomena are not considered in SANDYL. However, the estimated contribution to energy deposition due to effects such as induced currents and charge accumulation was negligible for our current density, risetime, gas pressure, and cell geometry.

In calorimeter calculations the code effectively provides the measured quantity, namely, the net energy dose from all sides, taking into account both gas and calorimeter backscatter. For gas deposition it calculates the detailed spatial distribution within the cell, information that is probably unobtainable by any other general method. However, to relate either type of calculation directly to experiment it is necessary to normalize computed and experimental calorimetry for some longitudinal position. This procedure basically determines the total incident beam energy for specified operating conditions.

In our SANDYL calculations to be described later we used a monoenergetic 235 keV beam incident on the foil. This value represents the average of the energy distribution determined from the diode voltage and current time dependence. The standard deviation of the energy distribution was less than 5 keV. Our monoenergetic assumption was justified by the fact that ± 5 keV beam energy variations did not significantly affect the SANDYL calculations of interest. We also neglected any initial transverse electron energy. This assumption was justified by the following considerations. The foil thickness was less than 15% of the Berger and Seltzer range so reasonable mean incidence angles would not change the effective foil thickness or energy lost in the foil significantly. Also SANDYL calculations with such a "cold" beam gave mean foil exit angles of about 40 degrees which is significantly larger than and, hence, insensitive to reasonable estimates of the mean angle of incidence. The input vertical profile on the diode side of the foil was iteratively adjusted with SANDYL to give self consistency between the calculated and measured profiles at the foil in the gas cell. The beam fluence measured at the foil by the calorimeters shown in Fig. 2B was found to be uniform within 10% error. Thus, the input vertical profile was taken to be independent of the horizontal transverse coordinate.

Figures 3 and 4 show the excellent agreement between experimental calorimeter fluence and SANDYL as a function of depth in argon at pressures of one and two atmospheres, respectively, for the five numbered vertical calorimeters shown in Fig. 2A. It is convincing to note that the same normalization constant was used for all ten curves shown in

Figs. 3 and 4. The small arrows along the horizontal coordinate axes indicate the positions of the SANDYL calculations. The curves are offset by the amounts indicated in order to present all five calorimeters on a single figure.

Having verified the reliability of SANDYL for our operating conditions we used it to calculate energy deposition in argon. Figure 5 shows longitudinal horizontal distributions at one and two atmospheres of argon. For comparison, 1-D Berger and Seltzer values are indicated by the horizontal dashes at the left. In the 1-D description these values would not change significantly across the box. The important point is that the Berger and Seltzer values would seriously overestimate the efficiency by a factor of three near the foil and such estimates are seen to be quite inadequate for reliable efficiency values. In the inset the broad dotted arrow and square show, to scale, the e^--beam height and cell cross section. The curves apply to the dotted 3-cm high strip across the vertical center of the cell. The dashed vertical lines across the figure indicate the region viewed by our optical system. Figure 6 shows the calculated vertical deposition profiles in this region. Note that the axes have the same relative scales as Fig. 5 and the vertical transverse profiles are relatively smooth compared to the longitudinal profiles of Fig. 5. The solid lines simply connect the SANDYL zone values whose standard deviations were typically about 7% for 64000 particles distributed over a (12.3 x 35) cm^2 model beam area.

By combining the optical techniques described above with experimentally normalized energy deposition calculations we have obtained the

fluorescence efficiency results shown in Table 1 at the indicated excited state densities.

The 1 atmosphere argon result is considered to be the most reliable since, in this case, the SANDYL energy deposition is least sensitive to the beam energy used. The overall combined statistical error in this result is estimated to be about ± 25%. For the other pure rare gas results the energy deposition calculation at 9 cm into the gas is more sensitive to beam energy and there is more potential for a systematic error. We would not expect a factor of two error in the worst case. Since the beam energy used in the calculations may have been somewhat high, we would expect the efficiency values given to be too low. The combined statistical error due to all other effects is again estimated to be about ± 25%. We intend to modify our cell to give a couple more optical axis locations closer to the foil. We will then repeat the higher pressure and heavier gas measurements.

The pure rare gas average excimer density values shown in Table 1 represent rough estimates. They depend on the ratio of triplet to singlet excimer density, N_3/N_1, and lifetime, τ_3/τ_1. The quantity $N_3\tau_1/N_1\tau_3$ was assumed to be negligible compared to one. The ratio N_3/N_1 depends in a sensitive fashion on the excitation conditions; however, we have used the statistical assumption $N_3/N_1 = 3$. The values shown were actually obtained by multiplying the total number of photons radiated per cm^3 by $4\tau_1/\tau_p$, where $\tau_p = 1$ μsec was the pulse length. If, instead, one were to assume $N_3/N_1 = 1$, the values would be a factor of two lower. For argon and krypton we used $\tau_1 = 4$ and 5 nsec, $\tau_3 = 3$ and 1 μsec, respectively.

We have also recently measured the fluorescence efficiency for a rare gas halide, namely, the $Ar/Xe/Br_2$ system. For the $XeBr^*$ thus formed, we assume a single radiative lifetime τ_r = 15 nsec and an average photon wavelength of 2800 Å. The exciplex density was then obtained by multiplying the total number of photons/cm^3 radiated by τ_r/τ_p. We have used this fluorescence to photolytically pump C_3F_7I and have obtained laser action on the well known 1.315 μ transition in atomic iodine. Figure 7 shows a typical gain switched pulse. The details of this work will be published elsewhere.[11]

In conclusion, we have demonstrated that one-dimensional energy deposition estimates can be seriously in error and that the three-dimensional SANDYL code can be used to get reliable gas deposition values. In addition, we have measured VUV fluorescence efficiencies in argon and krypton and found values in excess of 20 %. These values were obtained for excimer densities of about $10^{13}/cm^3$. We also measured the fluorescence efficiency of electron beam pumped XeBr and used its fluorescence to photolytically pump an iodine laser.

Acknowledgements

The substantial contributions of Leland G. Schlitt to effective utilization of the SANDYL code and many useful discussions in the course of this work are gratefully acknowledged. The authors thank Louis B. Rhodes for essential technical assistance, James C. Swingle, William Lai and associates for expert mechanical engineering design support, and also L. P. Bradley, E. V. George and R. R. Jacobs for valuable suggestions and encouragement. The accurate and timely VUV calibration of our detectors by Douglas M. Collins of Prof. Spicer's group at Stanford University and of our optics by Acton Research Corporation are very much appreciated.

References

1. J. Jortner, L. Meyer, S. A. Rice, and E. G. Wilson, J. Chem. Phys. 42, 4250 (1965).
2. E. E. Huber, Jr., D. A. Emmons, and R. M. Lerner, Opt. Comm. 11, 155 (1974).
3. G. S. Hurst, T. E. Stewart, and J. E. Parks, Phys. Rev. A2, 1717 (1970).
4. C. W. Werner, E. V. George, P. W. Hoff, and C. K. Rhodes, Appl. Phys. Lett. 25, 235 (1974) and Lawrence Livermore Laboratory, Rept. UCRL-77412 Preprint, submitted to Phys. Rev. A, Oct. 1975.
5. J. R. Murray and P. W. Hoff in Proc. Physics of Quantum Electronics (Crystal Mountain, Washington, July, 1973), Addison-Wesley, 1974.
6. J. R. Murray and C. K. Rhodes, Lawrence Livermore Laboratory, Rept. UCRL-51455, 1973.
7. S. D. Rockwood, O. P. Judd, and R. O. Hunter, Paper EB-3, 26th Gaseous Electronics Conference (Madison, Wisconsin, October, 1973); also Bull. Am. Phys. Soc. 19, 153 (1974).
8. S. D. Rockwood, Los Alamos Scientific Laboratory, Rept. LA-UR-73-1031, 1973.
9. M. J. Berger and S. M. Seltzer, "Tables of Energy-Losses and Ranges of Electrons and Positrons, in Studies in Penetration of Charged Particles in Matter, Nuclear Science Series Rept. # 10, NAS-NRC Pub. 1133 (National Academy of Sciences, Washington, 1964).
10. H. M. Colbert, SANDYL, Sandia Livermore Laboratory, Rept. SCL-DR-720109 (1973).
11. J. C. Swingle, C. E. Turner, Jr., J. R. Murray, E. V. George, and W. F. Krupke, (to be published).

Figure Legend

Fig. 1 Photographs of experimental hardware:

(a) Tantalum blade cold cathode in open diode chamber,

(b) Open gas cell with translatable calorimeter mount.

Fig. 2 Photographs of calorimeter arrays:

(a) Five calorimeter vertical array,

(b) Horizontal array of five parallel pair calorimeters.

Fig. 3 Comparison of SANDYL and calorimetry for argon at 1 atmosphere.

Fig. 4 Comparison of SANDYL and calorimetry for argon at 2 atmospheres.

Fig. 5 Longitudinal gas deposition profiles calculated by SANDYL in argon.

Fig. 6 Vertical gas deposition profiles calculated by SANDYL in argon along the optical axis.

Fig. 7 Rare gas halide pumped iodine laser pulse.

Table I Fluorescence efficiencies obtained to date in this investigation.

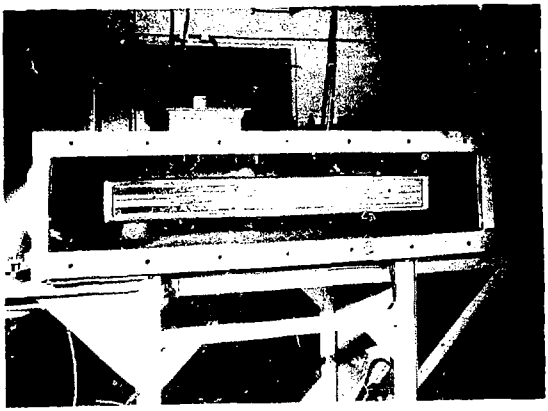

Fig. 1A

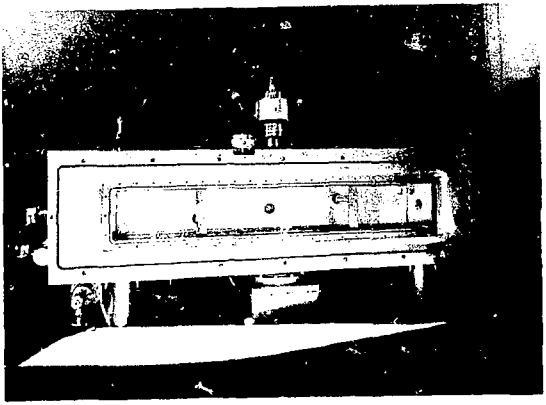

Fig. 1B

FIG. 1

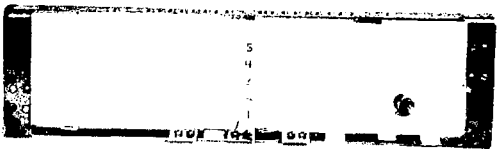

Fig. 2A

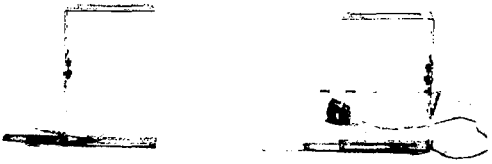

Fig. 2B

FIG. 2

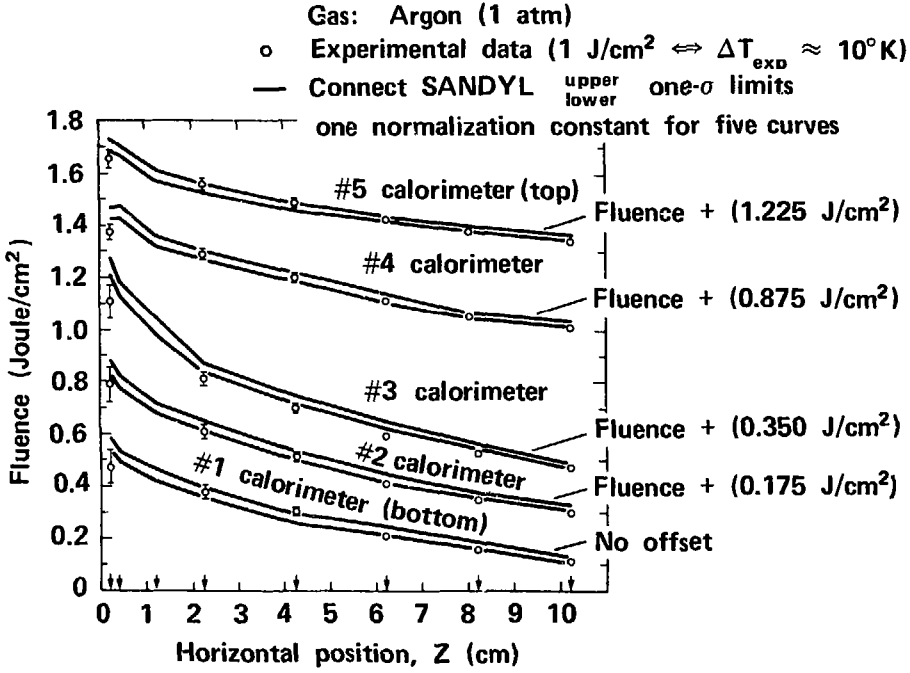
Gas: Argon (1 atm)
o Experimental data (1 J/cm² ⇔ ΔT_exp ≈ 10°K)
— Connect SANDYL upper lower one-σ limits
one normalization constant for five curves
#5 calorimeter (top)
Fluence + (1.225 J/cm²)
#4 calorimeter
Fluence + (0.875 J/cm²)
#3 calorimeter
Fluence + (0.350 J/cm²)
#2 calorimeter
Fluence + (0.175 J/cm²)
#1 calorimeter (bottom)
No offset
Fluence (Joule/cm²)
Horizontal position, Z (cm)
0
0.2
0.4
0.6
0.8
1.0
1.2
1.4
1.6
1.8
0 1 2 3 4 5 6 7 8 9 10

FIG. 3

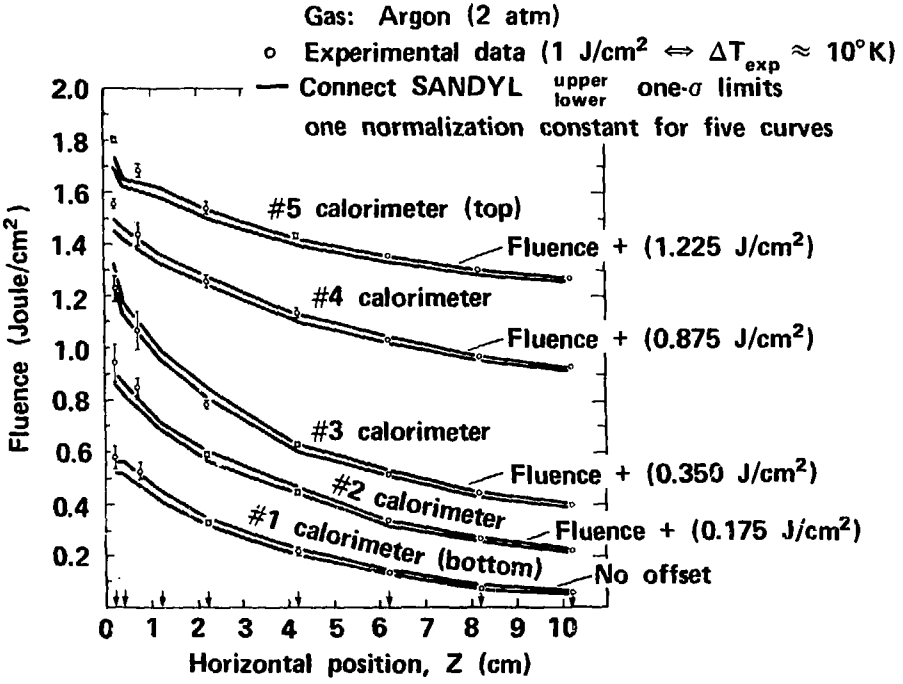
Gas: Argon (2 atm)
o Experimental data (1 J/cm² ⇔ ΔT_exp ≈ 10°K)
— Connect SANDYL upper lower one-σ limits
one normalization constant for five curves
#5 calorimeter (top)
Fluence + (1.225 J/cm²)
#4 calorimeter
Fluence + (0.875 J/cm²)
#3 calorimeter
Fluence + (0.350 J/cm²)
#2 calorimeter
Fluence + (0.175 J/cm²)
#1 calorimeter (bottom)
No offset
Fluence (Joule/cm²)
2.0
1.8
1.6
1.4
1.2
1.0
0.8
0.6
0.4
0.2
0 1 2 3 4 5 6 7 8 9 10
Horizontal position, Z (cm)

FIG. 4

Gas: Argon
Electron energy: 235 keV before foil
Foil: 25 micron titanium (1 mil)
Foil loss: ~30 keV

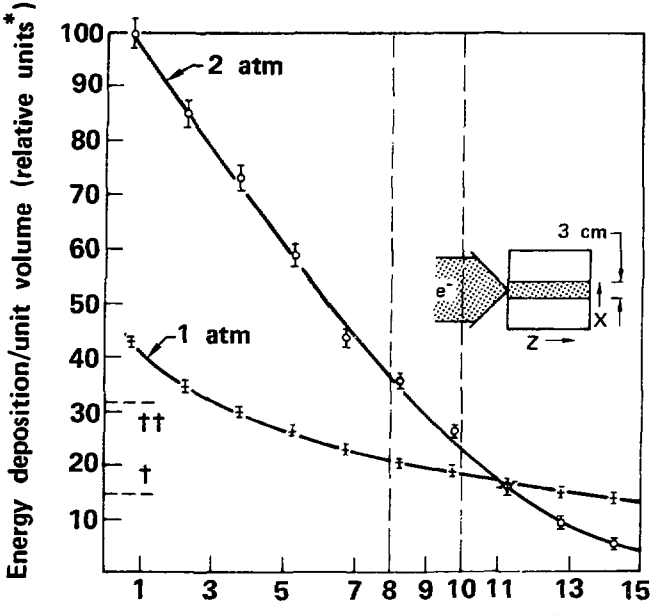

*100 r.u. ≈ 50 mJ/cm^3 ⟺ 2.5 Amp/cm^2 for 1 μsec
Berger & Seltzer † 1atm (Range ~ 40 cm)
†† 2atm (Range ~ 20 cm)

FIG. 5

Gas: Argon
Electron energy: 235 keV before foil
Foil: 25 micron titanium (1 mil)
Foil loss: ~30 keV

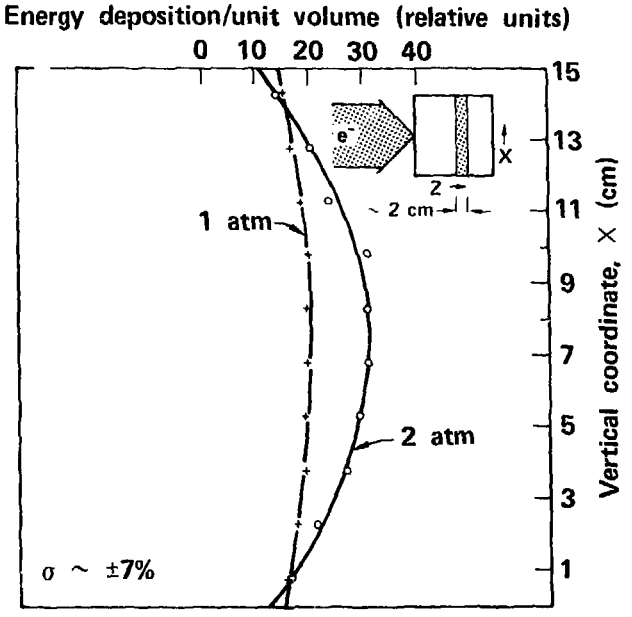

FIG. 6

IODINE LASER (1.315 μ)

Photolytic pumping at ~2800 Å via e-beam produced XeBr and/or Br_2 fluorescence

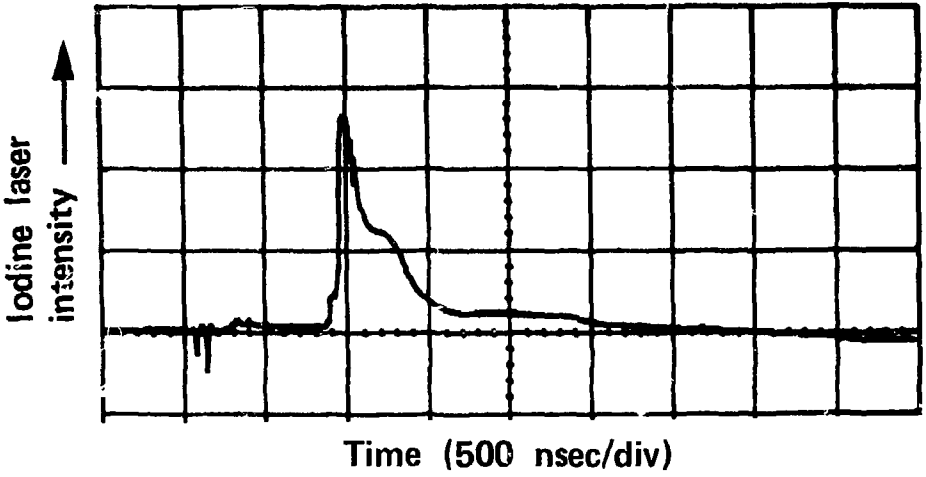

FIG. 7

TABLE 1

Gas	Pressure (Torr)	Efficiency (%)	~ Excimer Density (10^{13}/cm^3)	E_{rad} (mJ/cm^3)	E_{dep} (mJ/cm^3)
Ar	760	25	1.9	1.9	7.5
Ar	1520	21	1.9	2.0	9.6
Kr	760	22	1.7	1.2	5.5
Ar:Xe:Br_2	1500:25:1	~ 10	11	~ 5	44